CEA Comité Español de Automática

XLVI JORNADAS AUTOMÁTICA CARTAGENA 2025

UNIVERSIDADE DA CORUÑA

Jornadas de Automática

Inverse Kinematics Modeling of a Cable-Actuated Soft Robotic Neck in SOFA

Lipa, Gerson*, Rodríguez-Sanz, Alberto, Muñoz, Jorge, Martínez, Santiago, Monje, Concepción A.

RoboticsLab, Department of Systems Engineering and Automation, Universidad Carlos III de Madrid, Avda. Universidad, 30, 28911, Leganés, Spain.

To cite this article: Lipa, G., Rodríguez-Sanz, A., Muñoz, J., Martínez, S., Monje C.A. 2025. Inverse Kinematics Modeling of a Cable-Actuated Soft Robotic Neck in SOFA. Jornadas de Automática, 46. https://doi.org/10.17979/ja-cea.2025.46.12231

Resumen

Este trabajo presenta un estudio comparativo de dos enfoques para resolver la cinemática inversa de un cuello robótico blando accionado por cables. El primero se basa en un modelo analítico de curvatura constante, que asume una distribución interna y uniforme de los cables a lo largo de la estructura; esta hipótesis resulta inadecuada cuando los cables están fijados a una plataforma externa superior del robot, lo que genera desviaciones progresivas. El segundo método obtiene la cinemática inversa a partir de una simulación por elementos finitos acoplada con un solver de restricciones mecánicas en el entorno *Simulation Open Framework Architecture* (SOFA), lo que permite modelar con mayor fidelidad las interacciones físicas y las deformaciones reales del sistema. Los resultados obtenidos demuestran que la solución por simulación ofrece una robustez y una precisión significativamente superiores a las del modelo analítico cuando las suposiciones geométricas dejan de ser válidas, demostrando la eficacia de las herramientas de simulación física avanzada para el control de robots blandos en entornos y configuraciones complejas.

Palabras clave: Robótica blanda, Sistemas Bioinspirados, Modelado de Sistemas, Sistemas de Control No Lineales

Abstract

This work presents a comparative study of two approaches to solving the inverse kinematics (IK) of a cable-driven soft robotic neck. The first approach is based on a constant curvature analytical model, which assumes an internal and uniform distribution of cables along the structure; this hypothesis proves inadequate when the cables are fixed to an external platform at the top of the robot, leading to growing deviations due to cable sagging. The second method obtains the IK through a finite element simulation coupled with a mechanical constraints solver within the *Simulation Open Framework Architecture* (SOFA) environment, allowing for a more accurate modeling of the physical interactions and actual deformations of the system. The results demonstrate that the simulation-based solution offers significantly greater robustness and accuracy than the analytical model when the geometric assumptions are no longer valid, validating the effectiveness of advanced physical simulation tools for controlling soft robots in complex environments and configurations.

Keywords: Soft Robotics, Bioinspired Systems, Systems Modeling, Nonlinear Control Systems

1. Introduction

Soft robots have gained increasing relevance in recent years due to their ability to adapt to complex environments and the safety they offer in physical interactions with humans, which highlights their potential in biomedical and assistive applications. However, unlike traditional rigid robots, soft robots present unique challenges in terms of modeling, control, and simulation, due to their highly deformable nature.

One of the most common approaches to modeling the deformation of these systems is the *piecewise constant curvature*

*Corresponding author: glipa@ing.uc3m.es

(PCC) model, a geometric simplification that allows closed-form solutions for forward and inverse kinematics. However, this model presents significant limitations when applied to robots subjected to mechanical configurations or constraints not fully described by the model. These restrictions are present in the robotic neck studied in this work, in which the cables guiding the platform are located on the outside of the central structure. As a result, the assumptions associated with the model are no longer satisfied, leading to significant cumulative positioning errors.

More recently, more accurate physical models have been proposed that better reflect the curvature behavior of soft robots. Among these, approaches based on Cosserat rod theory and finite element formulations for continuum robots allow for the description of variable curvatures, axial elongations, and complex torsions along the robot (Renda et al., 2022; Bhalkikar et al., 2024; Bieze et al., 2018). These geometrically exact descriptions are usually inverted using iterative numerical methods which, although computationally more expensive, improve the accuracy of the inverse kinematics in cable-driven robots with multiple sections and arbitrary tendon paths. In this type of simulation, there is a trade-off between fidelity and efficiency: lumped models, simplified by segments, reduce computational cost and system accuracy, while continuous and FEM-based models offer greater precision but require more computation time. In general, advances in physical modeling have enabled more accurate solutions to the inverse kinematics of cable-driven soft robots by relaxing the assumptions of the piecewise constant curvature model, in exchange for using numerical techniques that allow the inversion of more complex models.

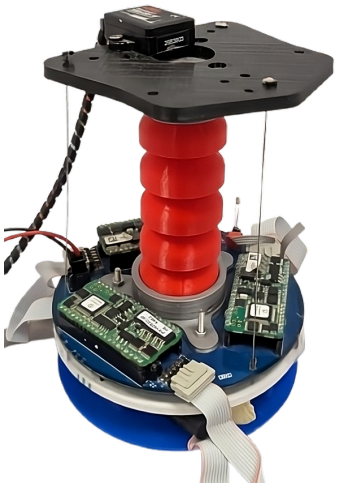

Figure 1: Robotic neck platform.

This study proposes an alternative for the IK analysis of the neck as described in (Nagua et al., 2018) using the piecewise constant curvature model. The soft structure consists of several links, each with an external diameter of 37 mm, connected and stacked through a central cylinder with a diameter of 27 mm. Together, these components form a total height of 100 mm. The platform is made up of three cables L_1, L_2, L_3 arranged equidistantly, separated by 120° around a circular section (see Figure 1), which actuate the neck to produce bending. Each tendon connects a lower rigid base with an upper rigid platform that integrates the *end-effector* and the inertial measurement unit (IMU). At rest, the cables have a length of 115 mm, which corresponds to the nominal distance between the base and the upper platform.

In this context, SOFA offers an integrated solution for simulating high-fidelity physics and solving inverse kinematics using finite elements and constraint solvers (Faure et al., 2012). SOFA allows precise modeling of the material's elastic properties, interaction with external cables, and kinematic constraints, all within a modular scene that integrates mappers and iterative solvers. This capability helps overcome limitations of traditional models, such as cable slack and nonlinear geometric effects, while maintaining robustness and accuracy superior to that of analytical methods.

The aim of this work is to compare the behavior of both approaches, the analytical piecewise constant curvature model and the numerical solution offered by SOFA[1], in solving the inverse kinematics of a soft robotic neck actuated by external cables. The results obtained allow assessing the feasibility of SOFA as a tool for controlling soft robots in scenarios where traditional analytical methods fall short.

2. Theoretical Foundations

2.1. Piecewise constant curvature model

The piecewise constant curvature model is a widely used approximation to describe the behavior of continuum soft robots based on a modification of the Denavit-Hartenberg parameters. Under this approach, the assumption that the neutral axis of the soft link bends within a single plane is made, maintaining a uniform curvature along the entire segment. Considering the robot has a total length L, the geometric state of a segment can be characterized by two parameters: the structure's bending angle α (inclination) and the angle β (top projection of the structure), which defines the orientation of the bending plane with respect to the base frame. The segment's curvature is then constant and defined as $\kappa = \alpha/L$.

The kinematics for obtaining the position of the robot's *end-effector* relative to the base frame is given by the following expressions (1), which correspond to the arc of a circle with radius $R = L/\theta$.

$$\begin{aligned} x &= R \cdot (1 - \cos\alpha) \cdot \cos\beta \\ y &= R \cdot (1 - \cos\alpha) \cdot \sin\beta \\ z &= R \cdot \sin\alpha \end{aligned} \tag{1}$$

For the homed position of the neck, when $\alpha \to 0$, the radius tends to ∞, and the robot adopts a straight configuration, leading to $(x, y, z) \to (0, 0, L)$.

Given the case of a robot actuated by n cables, where each cable i is located at a radial distance d from the neutral axis and positioned at an angle γ_i over the cross-section (see Figure 2), the elongation of each cable relative to its initial straight

[1]The code developed in this work can be found at: https://gitlab.com/softroboticslab/sofa-platforms.git

length L is described by equation (2). The final equality results from substituting $R = L/\alpha$, assuming an incompressible body whose total length does not change during deformation.

$$\begin{aligned}\Delta l_n &= L - (R - d \cdot \cos(\beta + \gamma_i)) \cdot \alpha \\ &= d \cdot \alpha \cdot \cos(\beta + \gamma_i)\end{aligned} \tag{2}$$

Figure 2 shows an schematic of the relationship between the variables used in the equation and their correspondence to the physical model of the robot.

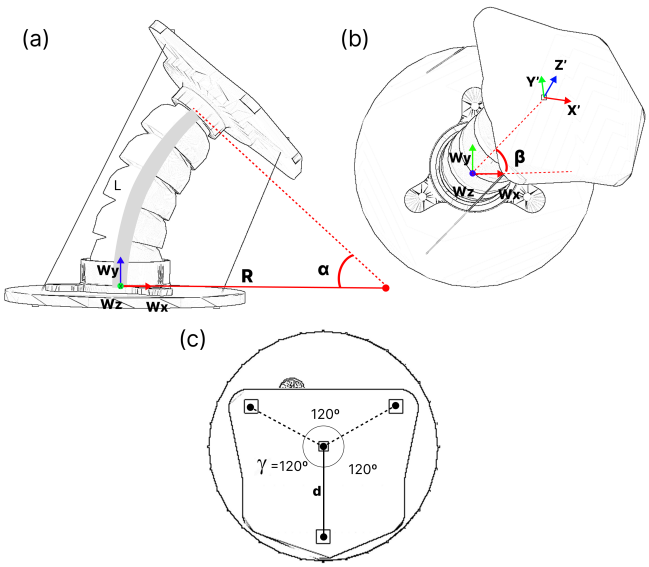

Figure 2: Schematic representation of the variables from the PCC model used in equation (2). (a) Lateral view displaying α angle. (b) Top view displaying β angle. (c) Top view displaying the placement of the cables.

Using equation (2), the displacements of each cable Δl_n can be calculated from the inclination parameter α and the orientation parameter β, obtained through robot sensors or predefined planning. These values are directly proportional to the positions the motors must rotate for controlling the robot to reach the desired position.

It is worth noting that, although the piecewise constant curvature model provides an efficient analytical representation, it presents certain limitations in real-life scenarios. In the system considered here, the externally placed cables loosen and deviate slightly during motion, introducing a mismatch between the theoretical curvature and the actual deformation of the robot. This deviation can lead to cumulative errors during sequential movements, ultimately affecting the model's overall accuracy.

2.2. SOFA: Architecture and Relevant Components

SOFA is an open-source simulator designed for finite element (FEM) simulation of deformable bodies, originally developed for applications in the medical field related to the deformation of soft tissues and organs. The FEM-based approach enables modeling the mechanical response of deformable materials subjected to displacements and external forces by finding approximate solutions to partial differential equations. As the name implies, the solution is achieved by reducing the problem into a set of smaller parts called finite elements. Its modular architecture is based on hierarchical scenes that allow flexible combination of physical objects, geometric representations, and resolution engines (solvers), all of which can be implemented or modified through the use of community or user created plug-ins. In (Coevoet et al., 2017) a set of tools were developed within SOFA to define and actuate deformable robots through different methods such as as cable-driven actuation, pneumatics, or the application of point or surface loads. The main components of a scene that define the simulation setup in SOFA are as follows:

- *MechanicalObject:* Defines the mechanical state of the system, including the positions, velocities, and accelerations of the nodes that make up the soft robot mesh.
- *TetrahedronFEMForceField:* Models the elastic behavior of the soft body using tetrahedral finite elements with a corotational formulation suitable for large deformations.
- *UniformMass:* Assigns mass to each node in the model, necessary to solve the system dynamics even in quasi-static simulations.
- *CableActuator and RestShapeSpringsForceField:* Simulate cable pulling actions through directed forces between specific points of the structure, indirectly controlling body deformation.
- *PositionConstraint:* Imposes conditions on the desired position of certain nodes, allowing inverse kinematics targets to be defined directly in physical space.
- *GenericConstraintSolver:* Resolves geometric constraints using iterative methods, adjusting control variables (such as cable lengths) until the imposed conditions are met.
- *ConstraintCorrection:* Applies corrections during each solver iteration to ensure physical consistency is maintained throughout the resolution process.
- *BarycentricMapping and LinearMapping:* Establish relationships between different levels of the model (e.g., from control points to physical nodes), propagating forces and motions across hierarchical structures.

One of the main advantages of FEM-based simulation over geometric models is its ability to represent unexpected behaviors, such as, structural torsion and compression, or cable sagging. This offers a more robust solution, but requires correct definition of the hyperelastic material properties and the model's meshes. The volumetric mesh can be generated from the surface model of the robot using external tools such as Gmsh or CGAL. This mesh is the main element that defines the computational cost of the simulation, so optimizing its design must be considered to achieve the desired accuracy while being able to run real-time simulations. Following the studies from (Lipa et al., 2025), a series of tests were carried in order to define the final number of tetrahedrons as 2363 and the Delaunay algorithm for the generation of the mesh.

The mechanical properties, such as the Young Modulus and the Poisson Ratio, of the material used in the

neck—thermoplastic polyurethane (TPU) with 82A shore hardness from the brand Recreus—were implemented based on the studies from (Rodríguez-Sanz et al., 2025) and (Xu and Juang, 2021), respectively. To compute the IK, the *end-effector* and the reference points shown in Figure 3 were used.

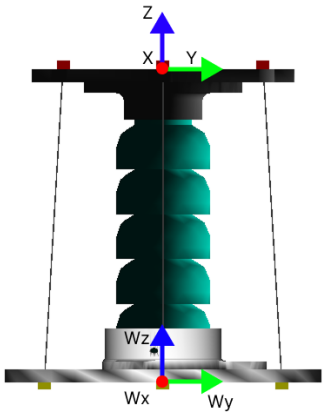

Figure 3: Reference frames used for the FEM-based solution of the *end-effector* and the origin.

Once the simulation environment is configured in SOFA, a command is given to the *end-effector* to reach a desired target angle. The inverse kinematics are then solved for the three cables, performing the required displacements, which are sent to the physical system through a ROS2 communication link.

3. Experimental Setup

To characterize the motion range of the robotic neck, three open-loop experiments were performed, covering the most favorable and the most unfavorable poses for the end effector of the platform. These were defined via the pitch and roll angles, which would later be measured using an IMU for a comparison between both the geometrical and the FEM-based approaches. The target angles for the experiments are gathered in Table 1.

Table 1: Target angle values for the experiments.

Angle (pitch, roll)	Description
44.4°, 0°	Describes a favorable movement, as the bending occurs in the direction of the tendon.
0°, 43.3°	Unfavorable movement, as it is oriented toward the middle zone of the cable arrangement (between 0° and 120°).
29.5°, 35°	Unfavorable movement combining bending and twisting, increasing the complexity of deformation.

For the PCC model approach, the following simplifications were made:

- The length of the soft link remains constant(incompressibility).
- The cables are perfectly vertical.
- The curvature is assumed constant, even with the cables placed externally to the soft structure.
- The vertical distance between the *end-effector* and the upper platform is considered negligible.

The first step is to map the target angles into the structure's inclination and orientation (α and β angles, respectively) by using equations (3) and (4). Following that, the displacements for each cable were obtained replacing the angles in equation (2).

$$\mathbf{n}_{Wz} = \begin{bmatrix} 0 \\ 0 \\ 1 \end{bmatrix}, \qquad \alpha = \arccos\left(\frac{\mathbf{n}_{Wz} \cdot \mathbf{n}_{z'}}{\|\mathbf{n}_{Wz}\| \, \|\mathbf{n}_{z'}\|}\right) \tag{3}$$

$$\mathbf{n}_{z'} = \begin{bmatrix} -\cos\phi \, \sin\theta \, \cos\psi + \sin\phi \, \sin\psi \\ \cos\phi \, \sin\theta \, \sin\psi + \sin\phi \, \cos\psi \\ \cos\phi \, \cos\theta \end{bmatrix}, \tag{4}$$

$$\beta = \arctan 2\left(n_{z',y}, \; n_{z',x}\right)$$

Conversely, for SOFA, a reference frame was defined for the *end-effector* to which the Euler rotations were applied. The simulation was configured to use a ramp signal as the input to generate a progressive angle variation until reaching the target position on the reference frame with a sampling time (dts) of 0.01 s for a total of 5 seconds. Meanwhile, the values of the cable displacements are measured at each time step.

Once the Δl_n values were obtained for both methods, the angles α_n were solved using equation (5) for each motor $n \in \{1, 2, 3\}$.

$$\sigma_n = \frac{\Delta l_n}{r_{\text{motor}}} \tag{5}$$

where $r_{\text{motor}} = 0.0065$ m is the radius of the motor winch [2].

Finally, the IMU measurements were recorded during the movements of the joint to the target angles to compare the positions reached with both methods. A schematic overview of this entire procedure is shown in Figure 4.The following section presents the results obtained from these measurements during the three experiments.

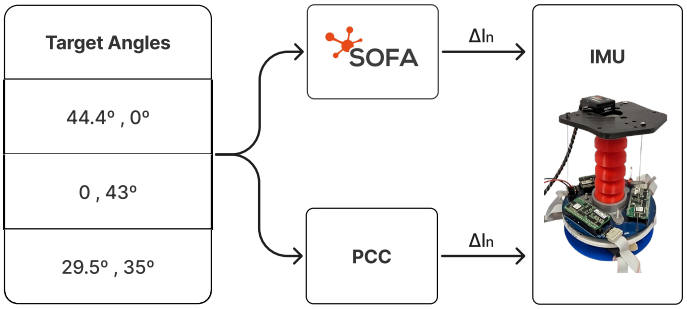

Figure 4: Schematic overview of the methodology employed for the experiments.

[2] In this case, α_n depends solely on the length variation Δl_n, not on the total length L of the tendon.

4. Results

In this section an evaluation and comparison of the results obtained from the experiments carried out, where different pitch and roll angles were given to the end effector to test the reachable poses for both methods. For each experiment the reached angle was compared to the target angles, after estimating the angle displacements obtained from the geometrical and the FEM-based methods.

4.1. Experiment 1: Pitch-axis bending

Figure 5 shows the results for the pitch angle, with a final target of approximately 43.3°. It can be observed that the SOFA simulation reaches the desired target quickly with a slight overshoot, while the PCC model shows a larger initial deviation, slowly stabilizing with a considerable steady-state error.

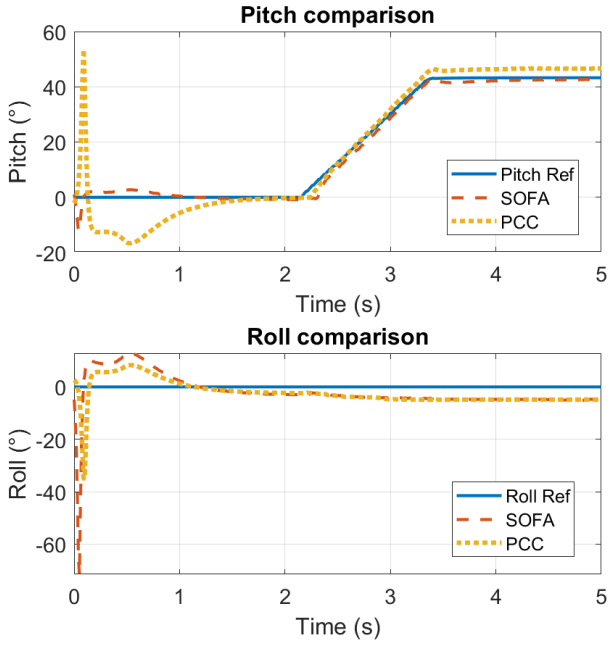

Figure 5: Measurements of pitch and roll angles using the IMU for the first experiment.

As for the roll angle, with a final reference of 0°, both methods show a significant initial overshoot, but eventually stabilize at values close to the reference value. This behavior is attributed to the lack of a homing strategy for the tendons.

4.2. Experiment 2: Roll-axis bending

In Figure 6, corresponding to the pitch angle with a reference of 0°, a significant deviation is observed in the piecewise constant curvature model with respect to the reference. The SOFA outputs, on the other hand, come closer to the target, although still with a notable error. These results once again highlight the lack of prior cable tension calibration for that position, as well as the need for a more precise tuning of the simulated model.

For the roll angle, with a reference of approximately −44.4°, both simulations exhibit similar behavior very close to the target, with effective stabilization after the initial transition.

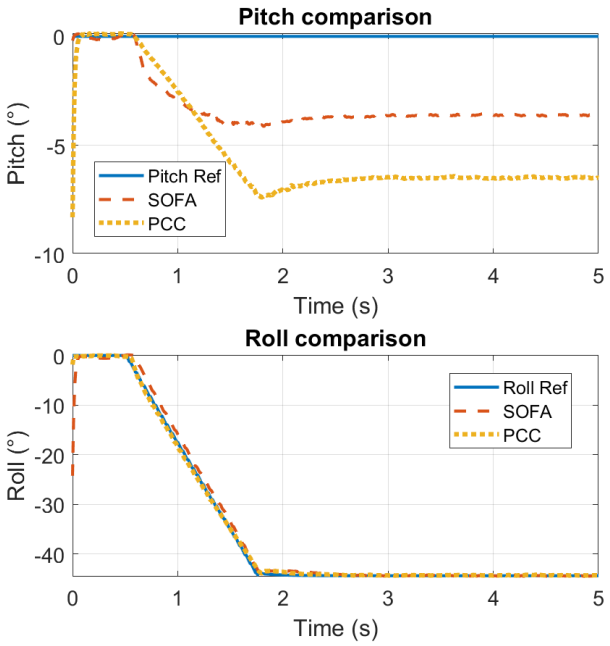

Figure 6: Measurements of pitch and roll angles using the IMU for the second experiment.

4.3. Experiment 3: Pitch and roll-axis bending

Finally, Figure 7 shows the results for the pitch angle, with a final reference of approximately 29.5°. Both approaches show effective stabilization, with the SOFA results being slightly more accurate in the final convergence.

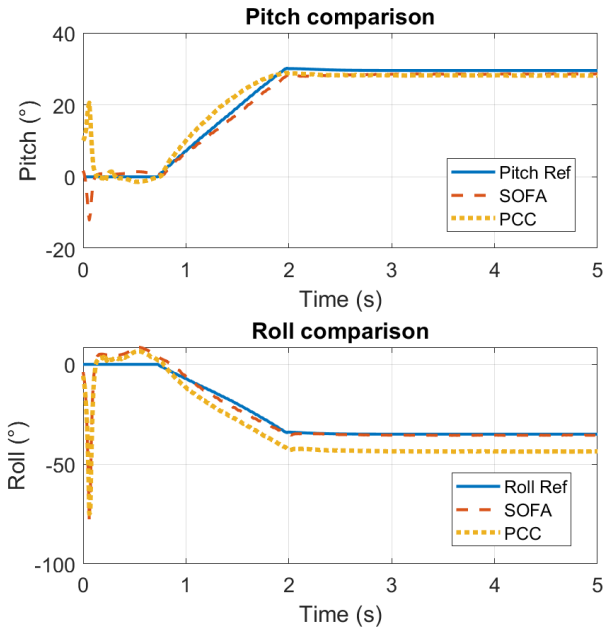

Figure 7: Measurements of pitch and roll angles using the IMU for the third experiment.

For the roll angle, with a final reference of around −35°, the SOFA results again demonstrate better final accuracy, although both models share a similar response during the initial transient phase.

Overall, SOFA simulations showed a better performance in reaching the target references, with consistently lower RMS errors in pitch and roll across the majority of experiments, as

summarized in Table 2. These results underline its potential as a tool for accurate simulation in soft robotics. Nonetheless, this improvement in precision is accompanied by a marginal increase in IK execution time (0.045 ms for SOFA versus 0.040 ms for PCC), which may be a consideration for real-time applications.

Exp. No.	Method	IK Time (ms)	RMS Pitch (°)	RMS Roll (°)
1	PCC	0.040	7.016	5.1344
	SOFA	0.045	1.7986	7.4181
2	PCC	0.040	5.7105	0.3917
	SOFA	0.045	3.3571	1.5623
3	PCC	0.040	2.7107	9.7343
	SOFA	0.045	1.5659	6.3668

Table 2: Comparison of IK time and RMS errors (°) for pitch and roll across experiments using PCC and SOFA.

5. Conclusions

The comparison of the three experiments shows that, although the analytical piecewise constant curvature model allows for fast and simple computations, its accuracy is limited as the target angles increase and the deformations become more pronounced. In contrast, the physics-based solver in SOFA succeeds in more faithfully reproducing the desired angles, achieving more precise and stable convergence across the full range of tests.

Nonetheless, it is important to qualify these results with some experimental and modeling considerations. The SOFA model was not calibrated with fully precise tuning of the parameters for the platform used, so part of the discrepancies may be attributed to that lack of refinement. Moreover, in the real platform, the tendons are not perfectly concentric around the soft structure nor do they remain fully vertical, as assumed by the piecewise constant curvature model. While the latter assumes a continuous curvature of the cables, in practice the tendons are only tensioned and do not curve around the soft body, as they run externally[3].

These factors introduce additional errors in both methods: on one hand, the SOFA solver could be improved by better adjusting geometry and anchoring conditions; on the other hand, the piecewise constant curvature model becomes inaccurate when its assumptions of curved and vertical cables are no longer valid.

Although SOFA demonstrates superior performance for complex postures, and the analytical model remains useful in simpler scenarios, the final choice should also consider the degree of achievable calibration and the actual geometric characteristics of the platform.

Future work will involve a more profound characterization of the material properties, focusing on the infill percentage and pattern, with the aim of more accurately representing the 3D printed soft neck in SOFA. In addition, the geometry and structural conditions of the system will be implemented more rigorously. Finally, a closed-loop control scheme will be developed using SOFA as the system model, with the goal of integrating it into more complex platforms and fully leveraging its physical simulation capabilities.

[3] https://vimeo.com/1088607551

Acknowledgements

The research leading to these results has been partially funded by the project ADAPTA, reference PLEC2023-010218, funded by MICIU /AEI /10.13039/501100011033; SIROCO, reference PID2023-147343OB-I00, funded by MICIU /AEI /10.13039/501100011033 and by FEDER, EU; and the R&D activity program with reference TEC-2024/TEC-62 and acronym iRoboCity2030-CM, granted by the Community of Madrid through the Directorate General for Research and Technological Innovation, under Order 5696/2024.

References

Bhalkikar, A., Lokesh, S., Ashwin, K. P., 2024. Kinematic models for cable-driven continuum robots with multiple segments and varying cable offsets. Mechanism and Machine Theory 200, 105701.
DOI: 10.1016/j.mechmachtheory.2024.105701

Bieze, T. M., Largillière, F., Kruszewski, A., 2018. Finite element method based kinematics and closed-loop control of soft, continuum manipulators. Soft Robotics 5 (3), 348–364.
DOI: 10.1089/soro.2017.0045

Coevoet, E., Morales-Bieze, T., Largilliere, F., Zhang, Z., Thieffry, M., Sanz-Lopez, M., Carrez, B., Marchal, D., Goury, O., Dequidt, J., Duriez, C., 11 2017. Software toolkit for modeling, simulation, and control of soft robots. Advanced Robotics 31, 1–17.
DOI: 10.1080/01691864.2017.1395362

Faure, F., Duriez, C., Delingette, H., Allard, J., Gilles, B., Marchesseau, S., Talbot, H., Courtecuisse, H., Bousquet, G., Peterlik, I., Cotin, S., Jun. 2012. SOFA: A Multi-Model Framework for Interactive Physical Simulation. In: Payan, Y. (Ed.), Soft Tissue Biomechanical Modeling for Computer Assisted Surgery. Vol. 11 of Studies in Mechanobiology, Tissue Engineering and Biomaterials. Springer, pp. 283–321.
DOI: 10.1007/8415_2012_125

Lipa, G., Rodríguez-Sanz, A., Muñoz, J., Martínez, S., Monje, C. A., 2025. Refinamiento de mallas para simulaciones en sofa framework: Equilibrio entre comportamiento dinámico y eficiencia computacional. In: Simposio de Robótica, Bioingeniería, Visión por Computador y Automática Marina. Accepted, unpublished.

Nagua, L., Muñoz, J., Monje, C. A., Balaguer, C., Sep. 2018. A first approach to a proposal of a soft robotic link acting as a neck. In: Actas de las XXXIX Jornadas de Automática. Área de Ingeniería de Sistemas y Automática, Universidad de Extremadura, Badajoz, Spain, pp. 522–529.
DOI: 10.17979/spudc.9788497497565.0522

Renda, F., Armanini, C., Mathew, A. T., Boyer, F., 2022. Geometrically-exact inverse kinematic control of soft manipulators with general threadlike actuators' routing. IEEE Robotics and Automation Letters 7 (4), 7311–7318.
DOI: 10.1109/LRA.2022.3183248

Rodríguez-Sanz, A., Sánchez, C., Martínez, S., Monje, C. A., 2025. Influencia de la orientación del patrón de relleno en las propiedades mecánicas del tpu de dureza 82A. In: Simposio de Robótica, Bioingeniería, Visión por Computador y Automática Marina. Accepted, unpublished.

Xu, Y.-X., Juang, J.-Y., 05 2021. Measurement of nonlinear poisson's ratio of thermoplastic polyurethanes under cyclic softening using 2d digital image correlation. Polymers 13, 1498.
DOI: 10.3390/polym13091498